Controlling adsorption and spin configurations of Co atoms on Si(111)-(7 × 7)

Qin Liu,[1,2] Guohua Zhong,[3] Fangfei Ming,[1] Kedong Wang,[1,4,*] and Xudong Xiao[1,3,†]

[1]*Department of Physics, The Chinese University of Hong Kong, Shatin, New Territory, Hong Kong, China*

[2]*Science and Technology on Surface Physics and Chemistry Laboratory, Mianyang 621907, China*

[3]*Center for Photovoltaic Solar Cell, Shenzhen Institutes of Advanced Technology, Shenzhen, China*

[4]*Department of Physics, South University of Science and Technology of China, Shenzhen, Guangdong 518055, China*

(Received 16 November 2013; revised manuscript received 5 March 2015; published 17 April 2015)

Combining scanning tunneling microscopy and first-principles calculations, we have shown that single Co atoms adsorbed on a Si(111)-(7 × 7) surface have eight different configurations that possess different spin magnetic moments. Despite the large adsorption energy, we have demonstrated that both the position and the spin state of single adsorbed Co atoms can be well controlled through the vertical atomic manipulation and the "*tip-touch*" operation that converts Co atoms among various adsorption configurations. Our approach to construct atomic-scale magnetic structures on a semiconductor surface can provide a new pathway to realize spin-based devices, including a scalable solid-state quantum computer.

DOI: 10.1103/PhysRevB.91.155417 PACS number(s): 75.75.Cd, 68.37.Ef, 68.43.Fg, 81.16.Ta

I. INTRODUCTION

Precise placement of a single dopant atom with net electron and nuclear spins on a semiconductor surface is a necessary prerequisite but long-standing problem for constructing a scalable solid-state quantum computer [1–4] and other atomic-scale spin-based devices [5–7]. Tremendous research has been dedicated to fabricate atomic-scale spin arrays [1,2,4,8] since the publication of the silicon-based quantum computer proposal in 1998 [3]. To date, the most successful technique to achieve such a goal is the so-called scanning tunneling microscope- (STM-) based hydrogen lithography [1,2]. This method circumvents direct manipulation of dopant atoms but suffers subsequent troubles, including how to avoid the diffusion of the incorporated atom when removing the hydrogen-resist layer at high temperatures. Although direct manipulation of an atom or molecule by STM seems a straightforward method to solve the problem, it unfortunately has not been realized because of the large adsorption energies of such atoms/molecules on a silicon surface [1,2,8]. Until now, only a few successful atom manipulation experiments have been achieved on a silicon surface at room temperature (RT) by atomic force microscopy, including vertical interexchange of Si-Sn atoms between tip apex and substrate [9], lateral manipulation of native Si adatoms [10,11], and assembling metal atom clusters by mechanical gate control [12]. Yet, conventional STM manipulation techniques, successfully demonstrated for atoms/molecules on smooth metallic surfaces [13–16], have obviously encountered serious challenges on semiconductor surfaces.

The motivation of our study is to find whether Co/Si(111) can be a potential system for constructing atomic-scale spin-based semiconductor devices, such as a quantum computer, etc. [1–7]. To achieve the goal of constructing atomic spin-based devices in a Co/Si system, three prerequisites [1,3,4,17–19] must be satisfied: First, single Co atoms adsorbed on Si(111)-(7 × 7) must have remaining net spins; second, Co atoms can be reproducibly manipulated on the surface; and last, if the Co atoms have various spin states induced by different couplings with a silicon substrate, these states must be controllably adjustable. To check whether the Co/Si(111)-(7 × 7) system can meet these three requirements, both the spin-related properties and the manipulations of single Co atoms, which were unexplored before, must be investigated.

We have first systematically studied all existing adsorption configurations of a single Co atom on Si(111)-(7 × 7) and refuted some points in an early study [20]. We have developed a new STM-based manipulation mode which can reproducibly manipulate *strongly bonded* magnetic atoms on a silicon surface and precisely transform their adsorption configurations. As a prototype, we demonstrated the successful precise placement of Co atoms on Si(111)-(7 × 7) first by a "*tip-touch*" operation to convert a single Co atom among various surface and *subsurface* adsorption configurations and then by a vertical atom manipulation to rearrange them into arrays with a carefully Si-modified STM tip. Combining with first-principles density functional theory (DFT) calculations [21,22], which reveal that the identified eight single Co atom adsorption configurations have different remnant spin magnetic moments, we, through manipulating the adsorption configurations, have effectively achieved precise and reproducible conversions among these spin states and constructed designed spin arrays of Co atoms. Our approach can not only provide a solution to construct scalable atom arrays for a solid-state quantum computer and other spin-related technologies [1–7,16,23], but also provide an indispensable tool to study basic physical phenomena on a semiconductor surface, such as substrate-induced magnetic anisotropy of individual atoms [24,25], Kondo effect [26,27], and magnetic atom coupling [15,28].

II. EXPERIMENTS AND METHODS

Our experiments were carried out with an Omicron variable temperature STM installed in an ultrahigh vacuum chamber with a base pressure better than 1×10^{-10} mbar. *N*-type Si(111) wafers with a RT resistivity of ∼0.026 Ω cm and a doping concentration of $7.3 \times 10^{17}/\text{cm}^3$ were used as the substrate. The substrate surface was cleaned to form

*Corresponding author: kdwang@phy.cuhk.edu.hk

†xdxiao@phy.cuhk.edu.hk

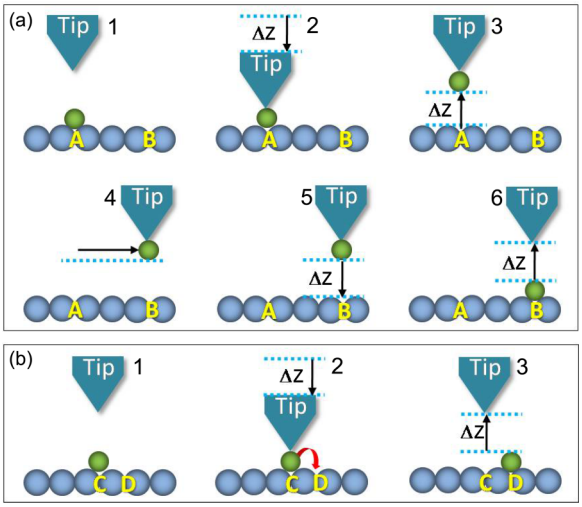

FIG. 1. (Color online) Schematic showing the basic steps for (a) vertical manipulation and (b) adsorption sites conversion, respectively, via the *tip-touch* method. The black arrow indicates the moving direction of the STM tip in each step. ΔZ is the approaching or retracting distance of the tip. $A-D$ represent different adsorption sites on the substrate.

Si(111)-(7 × 7) through a standard procedure [29] and a Co coverage up to ∼0.01 ML (monolayer) (1 ML = 7.83 × 10^{14} Co atoms/cm^2) were deposited onto the surface at RT by electron-beam evaporation. A tungsten tip was used for STM imaging and manipulation. In the manipulation experiments, two techniques, i.e., *tip-touch* operation and vertical manipulation, were used. Figure 1 shows the basic procedures in the two techniques. In the vertical manipulation [Fig. 1(a)], three stages, including the Co atom pick-up (1–3), translation (4), and drop-off processes (5 and 6), are achieved by applying various combinations of bias voltages and tip motions [30]. As shown in Fig. 1(a), the pick-up action involves three steps: (1) to move the tip above the target Co atom under normal scanning set-point condition and then switch the sample bias to +0.05 V, tunneling current to 5 pA, and turn off the feedback loop, (2) to vertically approach the tip towards the Co atom for a certain distance ΔZ. In this step, the atom may be transferred to the tip and stay on it. The result can be reflected by monitoring the tunneling current and subsequent image change, (3) to retract the tip back to normal imaging height and resume the feedback loop. In the translation stage (4), the tip is moved to a designated position under the normal scanning set-point condition. The last stage, dropping off the Co atom (5 and 6), consists of the same operations as the pick-up procedure, except for setting the sample bias to −0.05 V. In this stage, the Co atom is transferred from the tip back to the substrate. In order to obtain a tip which is suitable for manipulation, one needs to prepare it by tip crash into the sample surface [13,30]. The basic procedures of the *tip-touch* operation [Fig. 1(b)] are the same as the pick-up operation except without transferring the Co atom from the surface to the tip. Here, the STM tip is first placed at a designated position of the surface and then used to apply a mechanical force to the surface at a highly controlled advancing distance ΔZ to squeeze the Co atom from its original adsorption site to a nearby new adsorption site. The success of vertical manipulation and *tip-touch* operation rely on the properly chosen tip position, tip advancing distance, and especially the purposely modified tip apex. Since the basic procedures of vertical manipulation and *tip touch* are the same, how to immediately tell which one takes effect after the tip's action is important. As discussed in Ref. [30], two-state flipping signals in the I-Z spectrum taken in the tip-approaching process and the sudden changes in the subsequent STM images [also see Figs. 3(b) and 3(d)] always occur if a Co atom is successfully vertically transferred between the tip and the substrate. None of these two effects should occur in the *tip-touch* operation. So these two characteristics can be used to distinguish between vertical transfer of Co atoms and adsorption configuration conversions.

First-principles calculations based on DFT were performed to investigate the Co adsorption sites with the energies computed by the Vienna *ab initio* simulation package [21,22]. We employed the projector augmented-wave method [31] and the exchange-correlation functional with the generalized gradient approximation (GGA) [32] in the configuration optimization. The supercell was a slab consisting of one Co atom, six Si layers, and one H layer passivating the bottom surface. With the initial position of the Co atom properly chosen, the Co atom and the upper five Si layers were then relaxed until the residual forces become smaller than 0.02 eV/Å. The GGA + U method was further used to study the spin magnetic moment and the spin-polarized partial density of states (PDOS) of each Co adsorption configuration. One effective Hubbard parameter $U_{\text{eff}} = U - J$ with U and J representing the Hubbard repulsion and the intra-atomic exchange, respectively [33,34], was used in our calculations.

III. RESULTS AND DISCUSSION

A. Adsorption configurations of single Co atoms on Si(111)-(7 × 7)

Eight types of single Co atom adsorption configurations have been identified through comparing the topographic STM images before and after *in situ* Co deposition on Si(111)-(7 × 7). All these configurations were verified to contain only one Co atom as discussed later. Figure 2(a) displays the topographic STM images and simulated filled state images of a pristine faulted half unit cell (FHUC) and an unfaulted half unit cell (UHUC) of Si(111)-(7 × 7) for reference. Figure 2(b) shows the corresponding filled (A-H) and empty (A+ -H+) states STM images of each Co adsorption configuration. Based on their STM features and Ref. [20], we denote them as faulted pair (A), faulted center (B), faulted corner (C), faulted bright (D), unfaulted hopping (E), unfaulted center (F), unfaulted corner (G), and unfaulted bright (H), respectively. For instance, in a faulted pair configuration, two center Si adatoms equally dim in the filled state STM image. In a center/corner (B, C, F, and G) configuration, one center or corner Si adatom is much dimmer than the other Si adatoms in their corresponding half unit cells (HUCs). In the two bright configurations (D and H), three Si adatoms arranged in the shape of a triangle are brighter than their normal height contrast in the filled state STM images. By setting various initial Co positions, optimizing the configurations to obtain their adsorption energies, and simulating the respective STM images

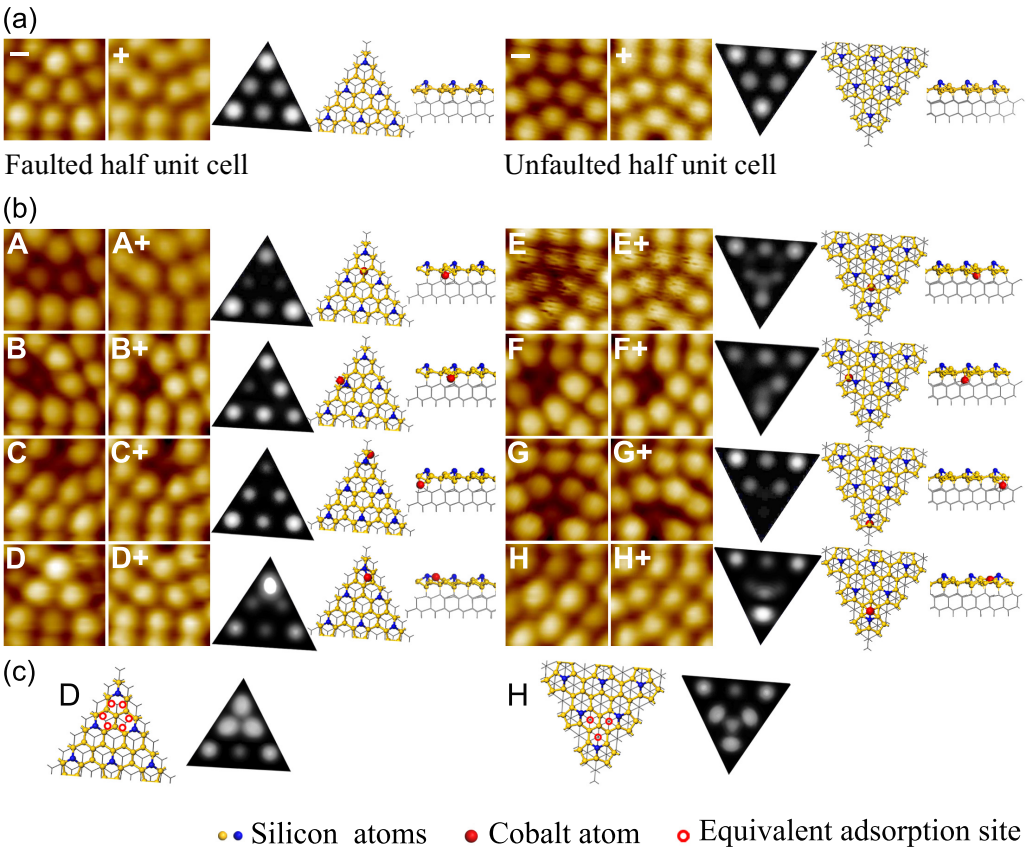

FIG. 2. (Color online) Filled state and empty state STM topographic images, simulated STM image, and structural models (top view and side view) of (a) clean Si half unit cells and (b) eight identified adsorption configurations of a single Co atom on Si(111)-(7 × 7). The filled and empty state images are indicated by "−" and "+," respectively, in (a). (c) The structural model showing six equivalent adsorption sites for configuration D and three equivalent adsorption sites for configuration H, respectively, in a basin (the area enclosed by a corner adatom and two nearby center adatoms in the same HUC [35]). The following images are the superposition of the simulated STM images of a Co atom at these equivalent adsorption sites. All the filled (empty) state STM images are taken at $V_s = -0.5$ V ($V_s = +1$ V) and $I = 5$ pA. The simulated images are taken at $V_s = -0.5$ V.

to compare with experimental observations, we have identified the Co adsorption site for each configuration. All the optimized configurations are also displayed in the structural model in Fig. 2(b) with their computed adsorption energies listed in Table I. The simulated filled state STM images ($V_s = -0.5$ V) which gives the assignment of the adsorption configurations are also displayed behind the experimental images in Fig. 2(b). The simulated images of configurations A, B, C, F, and G accurately reproduce the dimmed features of corresponding Si adatoms observed in the STM experiments. For example, the simulated image of faulted pair (A) contains two equally dimmed center adatoms, the simulations of configurations B, C, F, and G reveal a significantly dimmed center or corner adatom, and the simulation image of configuration F even reproduces the detail that two Si adatoms near the dimmed center adatom appear slightly brighter than their counterpart.

TABLE I. Adsorption energies E and spin magnetic moments M of eight identified single Co adsorption configurations obtained by DFT calculations.

		M (μB)							
Type	E(eV)	$U = 0$ eV	$U = 2$ eV	$U = 3$ eV	$U = 4$ eV	$U = 5$ eV	$U = 5.8$ eV	$U = 7$ eV	$U = 8$ eV
A	−6.18	0.02	0.05	0.16	0.92	1.10	1.19	0.83	0.90
B	−5.26	0.48	0.78	0.95	1.08	1.20	1.26	1.33	1.39
C	−5.68	0.00	0.01	0.01	0.52	0.72	0.97	1.21	1.31
D	−5.16	0.56	0.88	0.73	1.42	1.45	1.39	1.41	1.56
E	−5.71	0.06	0.71	1.07	1.24	1.39	0.84	0.93	1.01
F	−5.81	0.00	0.08	0.74	0.97	1.13	0.84	0.91	0.98
G	−5.84	0.00	0.09	0.69	0.86	0.98	0.88	0.96	1.04
H	−5.59	0.10	0.02	0.71	0.89	1.02	1.11	1.27	1.46

The differences between the simulated and the experimental images observed in configurations D, E, and H are caused by the fast hopping behavior of the Co atom as discussed below.

As shown in Fig. 2(b), most adsorption configurations show dark features in the STM images at both negative and positive sample biases (B, C, E, F, and G), and some of them show distinct features from the Si(111)-(7 × 7) background only at negative sample bias and small positive sample bias, i.e., <+0.6 V (A, D, and H). DFT calculations reveal that the dark configurations (A, B, C, E, F, and G) correspond to Co atoms adsorbed at the *subsurface* and the dark features are caused by charge transfer from the dangling bonds of Si adatoms to the nearby Si atoms. In contrast, the bright configurations (D and H) correspond to Co atoms adsorbed on the surface but still with a height lower than the outmost Si atoms. DFT calculations also indicate that the bright features are due to a charge transfer from the Si rest atom to the nearby Si adatom. The simulated image shows that only the Si adatom in close proximity to the Co atom appears bright, different from the experimentally observed feature. However, the given adsorption site in configurations D and H in Fig. 2(b) have other equivalent sites in the "basin" [35] as indicated by the red circles in Fig. 2(c). With the Co atom adsorbed on the outmost surface, it may frequently hop among these equivalent adsorption sites inside the basin at a very high rate [35] and result in a superposition of the simulated images for the Co atom at these equivalent sites. The superimposed images in Fig. 2(c) well reproduce the experimental features with three brightened Si adatoms. Configuration E, which appears only in the UHUC, corresponds to a hopping Co atom among three equivalent subsurface sites. The DFT optimized structural model of one of the three equivalent adsorption states is shown in Fig. 2(b). The simulated filled state image exhibits two obviously dimmed center adatoms and one slightly dimmed corner adatom. These features agree with the fact that the density of the black dots on center adatoms is higher than those on the corner adatoms. When imaged slowly, configuration E would appear as a dark "triplet" as mistaken by the early study [20]. Although, in general, many adsorbates were often observed to symmetrically adsorb on FHUC and UHUC due to the approximate mirror symmetry existing in the top two silicon layers in the dimer-adatom-stacking fault model [36], for Co atom adsorption, the DFT identified adsorption sites show noticeable asymmetry among faulted center, corner, pair, bright and unfaulted center, corner, unfaulted hopping, and bright adsorption configurations, respectively. This is because Co atoms stay deeply below the surface. They are more sensitive to the stacking fault existing between the third and the fourth silicon layers.

The images of dimmed center or corner adsorption configurations are very similar to the surface defect of a missing adatom. To demonstrate that dimmed center or corner configurations (B, C, F, and G) are indeed due to single Co adsorption instead of from a missing Si adatom, in a set of vertical manipulation operations in Fig. 3, we show an example of removing the Co atom in configuration G by transferring it to the STM tip and then re-depositing it back to form configuration B. Figures 3(c) and 3(d) clearly show that the UHUC is intact after the Co atom is transferred to the tip and the areas of images (b)–(d) taken with the Co atom on the STM tip show different resolutions from that with the clean tip. Similar pick-up and drop-off experiments have been repeatedly realized in all four dimmed center/corner configurations. So the manipulation experiment straightforwardly demonstrates that the observed dimmed feature in configurations B, C, F, and G is caused by the adsorption of a single Co atom.

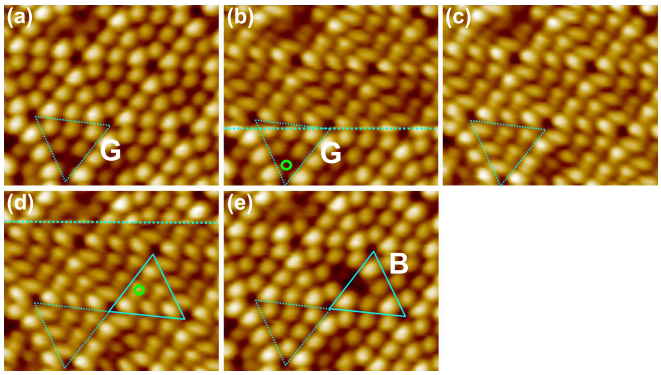

FIG. 3. (Color online) An example of vertical manipulation showing that configurations G and B contain only one single Co atom. (a) Image with configuration G in the dashed triangle before the Co atom was picked up. (b) and (c) Images depicting the Co atom being picked up and after pick-up from the position marked by the green dot. (d) and (e) Images exhibiting the Co atom being dropped off and after drop off on the green spot to form configuration B. The two dotted lines in (b) and (d) indicate when the pick-up and drop-off operations were performed.

B. Spin-related properties of single Co atoms on Si(111)-(7 × 7)

We performed theoretical calculations to study the spin-related properties of the adsorbed single Co atoms on Si(111)-(7 × 7). First-principles calculations show that single Co atoms on Si(111)-(7 × 7) have finite magnetic moments and the spin states for the eight Co adsorption configurations are different. Because of the strong correlation arising from the localized *3d* electrons in Co atoms, we have to apply the GGA + U approach to determine their spin magnetic moments [33,34]. Although the exact value of U_{eff} is not known, for a simple model of Co on Si(111)-(1 × 1) our theoretical estimation by following Refs. [37,38] results in $U_{\text{eff}} \sim 5.8$ eV, which can serve as a good reference. In the following we used various U_{eff}'s to calculate the magnetic moment and the PDOS for each adsorption configuration. As shown in Table I, if we neglect the correlation effect ($U_{\text{eff}} = 0$), most configurations except B and D are nonmagnetic. If we gradually increase U_{eff} from 0 to 5.0 eV, the spin magnetic moments of all configurations increase, and all eight configurations become magnetic when U_{eff} reaches 4.0 eV. For configurations $D-G$, their magnetic moments reduce slightly at $U_{\text{eff}} = 5.8$ eV but recover the increased trend with a further increase in U_{eff} from 5.8 to 8.0 eV. Similarly, the magnetic moment of configuration A slightly decreases at $U_{\text{eff}} = 7.0$ eV but increases again at $U_{\text{eff}} = 8.0$ eV.

As demonstrated by the calculated spin-polarized PDOS curves, it is the exchange splitting in d orbitals that gives rise to the magnetic moments and the Co-s and -p orbitals do not

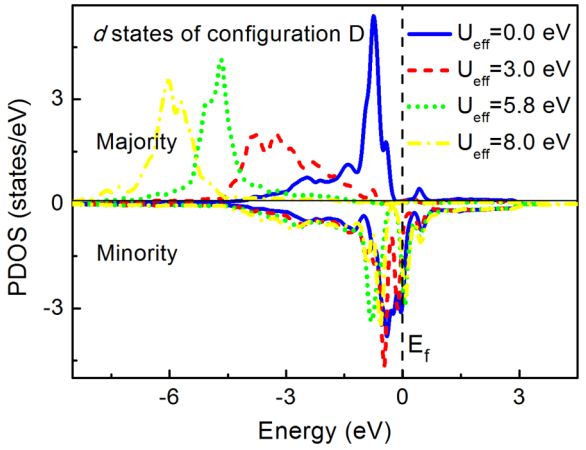

FIG. 4. (Color online) Calculated spin-polarized partial density of states for the d orbitals of configuration D at various U_{eff} values. For clarity, the majority and minority states are displayed as positive and negative values, respectively.

make any contribution as expected. To further elaborate the origin of the spin magnetic moment and the effect of varying U_{eff}, we plot the calculated PDOS for the spin-polarized d orbitals of configuration D at $U_{\text{eff}} = 0, 3.0, 5.8, 8.0$ eV in Fig. 4. At $U_{\text{eff}} = 0$, the occupation of spin-up (majority) and spin-down (minority) states is already nonsymmetric and results in a net spin magnetic moment. When U_{eff} is increased to 3.0 eV, the majority d states are pushed towards the lower-energy region whereas the minority d states do not undergo any obvious shift. Since the majority d states locate in the same energy range as the Si extended p states of -4 to -1 eV, they become strongly hybridized and broadened. The obvious energy splitting in the minority d states is due to the opposite shifts of the d_{xy} state (pushed towards the Fermi level) and the d_{yz} state (pushed away from the Fermi level). Here, x, y, and z represent $[11\bar{2}]$, $[\bar{1}10]$, and $[111]$ directions, respectively. At $U_{\text{eff}} = 5.8$ eV, the majority d states are further pushed to the energy region below -4 eV, and the hybridization with the delocalized Si-p states is weakened, resulting in a localized majority d peak. In contrast, the splitting in d_{xy}, d_{yz}, and d_{zx} states becomes larger, and the minority d states get even less filled. This increases the spin magnetic moment. Similar variations in the spin-polarized d states with an increasing value of U_{eff} are also observed in other configurations. When U_{eff} is increased from 5.8 to 8.0 eV, the majority d states are obviously pushed to an even lower-energy region (below -5.0 eV), whereas the occupied minority d states slightly shift towards the Fermi level. Compared with the results at $U_{\text{eff}} = 5.8$ eV, the slight enhancement of the magnetic moment at $U_{\text{eff}} = 8.0$ eV mainly originates from the less filling in the minority d_{z^2} orbital. In general, increasing U_{eff} enhances the exchange splitting in d orbitals and results in larger spin magnetic moments. The reduction of magnetic moment of configurations E, D, F, and G from $U_{\text{eff}} = 5.0$ to $U_{\text{eff}} = 5.8$ eV and configuration A from $U_{\text{eff}} = 5.8$ to $U_{\text{eff}} = 7.0$ eV is due to the fact that the minority d states are also pushed to the lower-energy region, resulting in higher occupation and thus a smaller net spin moment. Further increasing U_{eff} to 8.0 eV, some minority d suborbitals become less filled, leading to a slight increase in the magnetic moments. The existence of finite spin magnetic moments for the above eight Co adsorption configurations at various given U_{eff} values was in strong contrast to bulk $CoSi_2$ and CoSi for which the null spin magnetic moment was always found by calculations independent of U_{eff}. This agrees well with previous experimental results for 1.4–2.1-ML Co films on the Si(111) surface where cobalt disilicide is formed at the interface [39,40]. Therefore, we confirm that the use of U_{eff} in the above theoretical calculations does not introduce any artificial effects.

Although around $U_{\text{eff}} = 5.8$ eV all the eight adsorption configurations have finite spin magnetic moments (Table I), the origins of their spin moments are different. To clarify it, we have displayed the computed spin-polarized density of states for five d suborbitals for each configuration in Fig. 5. For all eight configurations, the majority d states are pushed to the lower-energy region, whereas the splitting of the minority d states is increased when U_{eff} is increased to 5.8 eV. For configuration A, the magnetic moment at $U_{\text{eff}} = 5.8$ eV originates from the less filling of minority states caused by the splitting among d_{xy}, d_{yz}, and d_{zx} states. For configuration B, the splitting in minority d_{yz} and d_{zx} states results in a

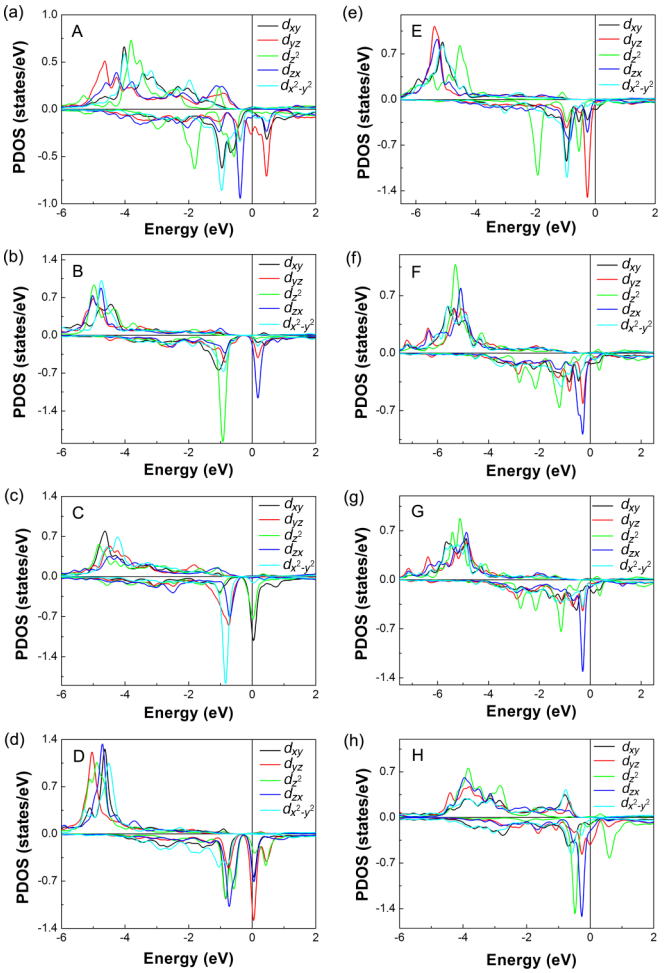

FIG. 5. (Color online) Calculated spin-polarized density of states of five d suborbitals for configurations $A-H$ at $U_{\text{eff}} = 5.8$ eV.

large net spin magnetic moment. For configuration C, the spin magnetic moments originate from the splitting in the minority d states caused by the shifts in the d_{z^2} and d_{xy} states (pushed above the Fermi level). For configuration E, the spin magnetic moments at $U_{\text{eff}} = 5.8$ eV originate from the difference of fully occupied majority d states and partially occupied minority d_{xy} and $d_{x^2-y^2}$ states. For configuration F, the spin magnetic moments are mainly ascribed to the small amount of unoccupied minority d_{z^2} and d_{xy} states and the almost fully occupied majority d states. For configuration G, the full occupation of the majority d states and some unoccupied minority d_{z^2}, d_{zx}, and d_{xy} states together contribute to a finite spin magnetic moment. For configuration H, the spin magnetic moment is mainly caused by the obvious increased splitting in the minority d_{z^2} states. To summarize, at our estimated value of $U_{\text{eff}} = 5.8$ eV, the eight adsorption configurations of single Co atoms on Si(111)-(7 × 7) are magnetic, and each configuration represents a spin state with different spin magnetic moments.

C. Controllable adsorption/spin state conversions by the tip-touch method

To facilitate applications in quantum computer and other spin-based technologies, it is desirable to have identical spin states from the Co atoms adsorbed at designated sites. As shown before, different adsorption configurations of single Co atoms represent different spin states with certain spin magnetic moments. With Co atoms adsorbed in different configurations after thermal deposition on Si(111)-(7 × 7), we must be able to convert them into a given configuration, and even the Co atom is adsorbed in the same HUCs. We here have applied the *tip-touch* method to successfully "tune" the spin states of single Co atoms through adsorption configuration conversions.

In Fig. 6 we show four examples of tip-induced Co adsorption configuration conversions. With the tip positioned above the middle of three center Si adatoms of the UHUC [Fig. 6(a)] for the *tip-touch* operation, the unfaulted bright configuration H could be converted into the unfaulted corner configuration G. The reverse was also realized and shown in Fig. 6(b) by positioning the tip right on the corner dark atom for the *tip-touch* operation. Similarly, reversible conversions among unfaulted center and unfaulted bright configurations were also realized by this method (not shown here). Figures 6(c) and 6(d) depict that an unfaulted hopping Co atom (configuration E) was converted into an unfaulted center configuration F or forced to a nearby FHUC to form a faulted pair configuration A. The mechanism of the *tip-touch* mode is different from the vertical manipulation used in the next section (Sec. III D) and the vertical atom interexchange used in Ref. [9]. In the *tip-touch* mode, no vertical transfer of the targeted atom occurs between the Si substrate and the tip apex. In the examples shown in Fig. 6 for the *tip-touch* operation, the targeted atom is forced from its original adsorption site into a nearby site on Si(111)-(7 × 7) by the approaching STM tip without leaving the Si surface. In contrast, the targeted atom adsorbed on the substrate is exchanged with an atom originally on the tip apex in the manipulation mode of Ref. [9], and there is one and only one atom vertically transferred between the tip apex and the substrate surface in our vertical manipulation mode presented in Sec. III D.

Many other conversions were achieved as well. For the sake of simplicity, we give a schematic in Fig. 7 to outline all 14 kinds of experimentally realized conversions with their respective conversion directions and the *tip-touch* positions labeled by the same numbers. Most conversions are reversible. However, configuration A is very hard to be converted into

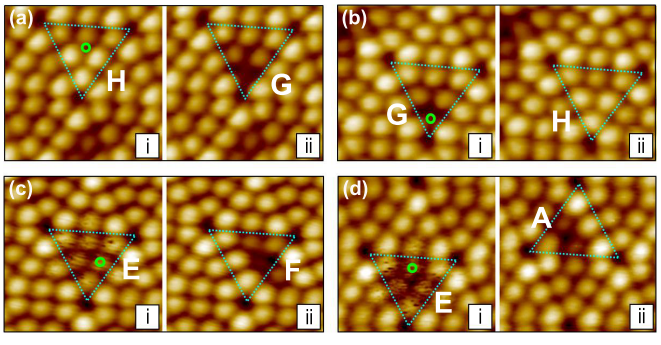

FIG. 6. (Color online) (a)–(d) Four sets of STM images showing adsorption configuration conversions realized by the *tip-touch* operation. In each example, panels (i) and (ii) show the image before and after the conversion, respectively. The triangles mark the corresponding Co adsorbed HUCs. The green dots indicate the tip position in the *tip-touch* operation. The uppercase letters near the triangles in each panel indicate the adsorption configuration of the Co atom. The images are taken at $V_s = -0.5$ V and $I = 5$ pA.

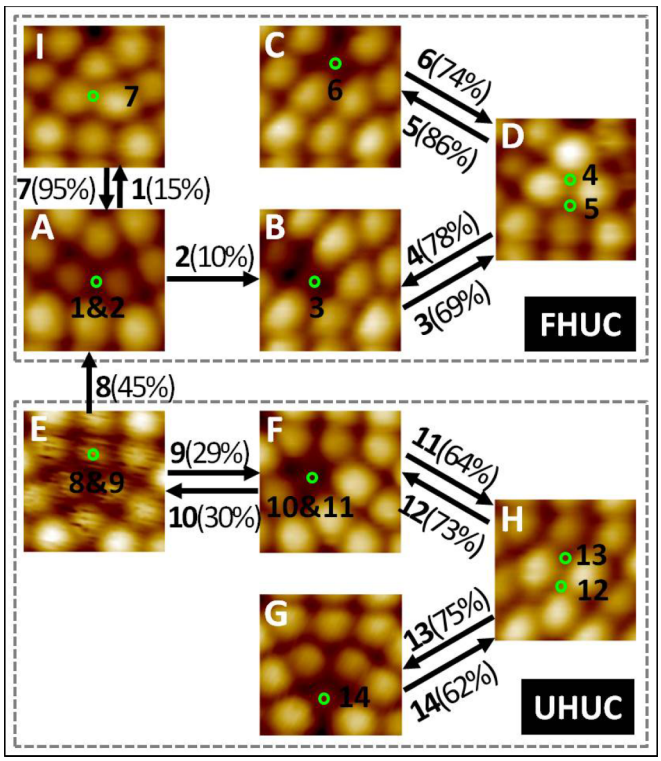

FIG. 7. (Color online) Schematic of all 14 types of realized adsorption configuration conversions. Black arrows indicate the directions of conversion with labeled numbers near the green dots for the *tip-touch* positions and near the arrow for the conversion type. The success rate of each conversion is shown in parentheses.

other configurations except a metastable configuration I, which is also shown in Fig. 7 and can be converted back into configuration A immediately by the *tip-touch* operation or spontaneously after a few minutes at RT. In our experiments, configuration A has been converted to configuration I with a success rate of ∼15%. In addition, configuration A can be converted to its other two equivalent adsorption sites in the same FHUC, i.e., a dimmed pair in a different arrangement, with a success rate of 26% (not shown in Fig. 7). Although we have successfully converted configuration A into configuration B a number of times, the success rate of ∼10% is much lower than the other conversions. Moreover, the conversion from configuration A to configuration E (hopping atom) has never been realized. Based on these observations, we infer that configuration A is very stable and has a large adsorption energy, supporting the DFT calculation results that configuration A has the largest adsorption energy among all adsorption configurations (Table I). Our experiments above have not only demonstrated that nearly all the identified single Co adsorption configurations can be converted to each other directly or indirectly by the *tip-touch* operation, but also proved that these eight adsorption configurations all contain only a single cobalt atom. More important is that we in fact realized the conversions among different spin states via the tip-induced adsorption configuration conversions since each configuration represents a different net spin.

For the success of the *tip-touch* method, one must choose the proper parameters in order to achieve the desired conversion. Three parameters determine the result of the *tip-touch* process: the position of the STM tip, the states of the tip apex, and the tip approaching distance (ΔZ). Generally speaking, the absolute value of ΔZ in each kind of conversion is different. The required value of ΔZ depends on the vertical position of the Co atom in the substrate and the interaction strength between the tip and the Co atom. The tip position and the states of the tip apex, including the shape, chemical properties, etc. [13], together determine the type of the conversion. For example, configuration D can either be converted into configuration B or configuration C, depending on the tip positions, as shown by green circles 4 and 5 in Fig. 7. Once the states of the tip apex change, the resulting configurations will be different even if the tip is placed at the same position. Conversions 8 and 9, which result from placing the tips with different properties at the same position give an example to illustrate this point. To obtain a suitable tip-apex state for a designated conversion, we need to prepare the tip by applying repetitive voltage pulse or gentle "tip-crash" treatments. Yet, the exact states of the tip apex (atomic structure) for those conversions remain unknown. For most conversions, their success only depends on the lateral tip position and the tip approaching distance ΔZ. There is no special requirement on the states of the tip apex. As shown in Fig. 7, the conversions among dimmed center, corner, and bright configurations (conversions 3–6 and 11–14) all have a high success rate beyond 60% with properly chosen ΔZ and tip position (indicated by the green circles) in the *tip-touch* operation. Other than conversions 1 and 2 discussed above, conversions 8–10 also have a relatively low success rate of 45%, 29%, and 30%, respectively. These conversions require special states of the tip apex, and the tip apex is easily altered in the repetitive *tip-touch* operation, leading to a different type of conversion. Nevertheless, if we consider the sum of the success rate of conversions 8 and 9 (or conversions 10 and 11), the rate goes as high as 74% (94%). From the above statistics, we observe that most of the tip-induced conversions in Fig. 7 have good reliability and repeatability.

D. Vertical manipulation of a single Co atom

In order to construct useful magnetic structures, we often require an array of identically adsorbed magnetic atoms periodically positioned in space. As suggested in the proposal for a silicon-based quantum computer [3], atoms carrying spins must be placed into the material in an ordered array and separated by proper distances. Only the *tip-touch* operation cannot meet the requirement of fabricating ordered atom arrays. A vertical manipulation mode must be used to reposition Co atoms freely on the surface. Through carefully optimizing various conditions, the single Co atoms in some adsorption configurations can be successfully picked up and dropped off on the Si(111)-(7 × 7) surface.

In Fig. 8 we show four examples of repositioning a single Co atom via vertical manipulation. As shown in Figs. 8(a) and 8(c), to pick up a Co atom in a dimmed corner or center configuration, one must position the tip above the dimmed Si adatom in the pick-up procedure. In the drop-off process, one can obtain different adsorption configurations through choosing a proper position for the tip. If the tip is positioned above the center or corner Si adatom, one can obtain a dimmed center (B, F) or corner (C, G) configuration. Otherwise, if the tip is placed above the Si rest atom, one can obtain a bright configuration D or H. For example, when the tip was aimed right above the Si adatoms in the drop-off process in Figs. 8(a) and 8(c) [marked by the pink circle in panel (ii)], a dimmed center or corner configuration was obtained. In Figs. 8(b) and 8(d), when the tip was placed above the Si rest atom site in the drop-off process, a bright configuration H was obtained. This conclusion was applicable to both FHUC and UHUC.

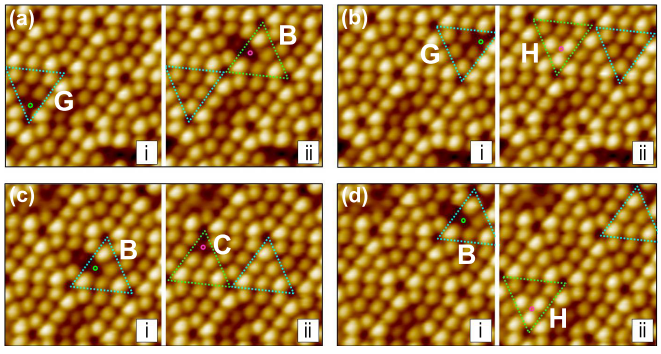

FIG. 8. (Color online) (a)–(d) Four examples of vertical manipulation of a single Co atom on Si(111)-(7 × 7). Panels (i) and (ii) show the images before picking up and after dropping off the Co atom, respectively. The dotted blue triangles enclose the HUC where the Co atom stays before pick-up. The green dotted triangles enclose the HUC where the Co atom is put down. The uppercase letters near the triangles in each panel indicate the configuration of the Co atom. The green and pink circles represent the position of the tip in pick-up and drop-off processes, respectively. The images are taken at $V_s = -0.5$ V and $I = 5$ pA.

Besides, we found that the Si HUCs [enclosed by the dotted blue triangle in panel (ii) of each example] were not damaged and remained intact after we removed the Co atom.

In contrast to many other adsorbates with low adsorption energy, including a Ag atom on Si(111) with only 2.4 eV [30,35], manipulating a *strongly bonded* atom, such as Co on a *rough* Si(111)-(7 × 7) surface with an adsorption energy of 5.2–6.2 eV (Table I) imposes a big challenge, especially when picking it up from the surface in the vertical STM manipulation. To overcome this challenge, we must first modify the tip apex by repetitively gentle crashing the tip on the clean Si(111) until it becomes capable of picking up Co atoms. We speculate that some Si atoms are attached to the tip apex in this procedure so that the modified tip apex can provide a similar potential environment as the Si(111) surface to trap a Co atom. After enormous repetitive tip-crashing experiments, we found only about 15% of the tips could produce stable repeatable vertical transfer of a Co atom between a tip apex and a Si substrate. But once the tip apex is properly modified, the success rate of vertically manipulating the Co atom (in configurations B, C, F, and G) is above 60% with optimized parameters. Second, we have to approach the tip apex very close to or even touch the Co atom for the pick-up. This is achieved by setting a very low sample bias of +0.05 V, about one order of magnitude smaller than that used in manipulating a Ag atom on Si(111) [30].

Yet, we found that among the eight configurations in Fig. 2(b), only the dimmed configurations B, C, F, and G can be directly picked up by a STM tip even with all conditions maximally optimized. The rest of the four configurations A, D, E, and H cannot be directly picked up. Fortunately, as shown in Figs. 6 and 7, we can realize the conversions among different adsorption configurations by the *tip-touch* method. In order to pick up Co atoms in other configurations, we must combine the vertical manipulation and the *tip-touch* techniques. Figure 9 shows an example of picking up a Co atom in the bright configuration H by combining the two methods. Since the bright configuration H in Fig. 9(a) cannot be directly picked up by the STM tip, we first convert it to the unfaulted corner G configuration in Fig. 9(b) via *tip touch*. Then we pick up the Co atom from configuration G [Fig. 9(c)] and set it into a faulted center configuration in the neighboring FHUC [Fig. 9(e)]. One can obtain different Co configurations through choosing a proper tip position in the drop-off process of vertical manipulation. Alternatively, we can also vary the adsorption configuration via *tip touch* after putting down Co atoms on the silicon surface.

E. Fabricating Co atom arrays carrying identical spins

Apparently, via the combined vertical manipulation and the *tip-touch* method, we can control both the position and the spin states of a single Co atom on the Si(111)-(7 × 7) surface. It implies that we can construct designated atomic-scale structures with given spin states, which is a prerequisite of fabricating a semiconductor-based quantum computer [1–4] and other cutting-edge spin-based devices [5–7]. Here, we give an example to show our capability of constructing Co atom arrays carrying identical spins on a silicon surface. As shown in Fig. 10(b), we have successfully set five Co

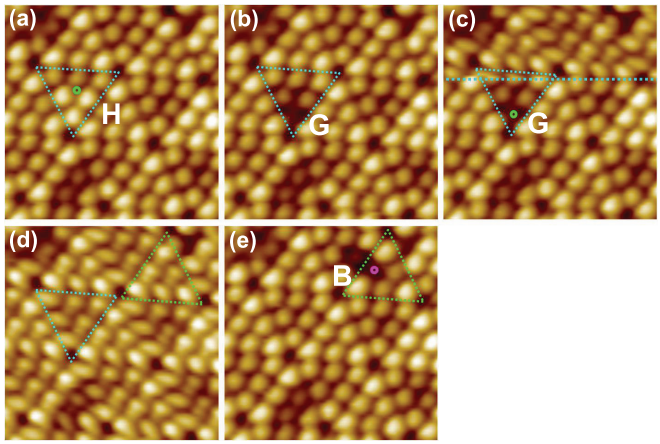

FIG. 9. (Color online) An example of combined use of adsorption configurations conversion and vertical manipulation. (a) and (b) STM images of converting a Co atom (enclosed by the dotted blue triangle) from configuration H to configuration G by the *tip-touch* operation. The green circle indicates the tip position in the *tip-touch* operation. Panel (c) shows the image of picking up the Co atom in the dotted triangle. Panel (d) shows the image scanned by the STM tip within an extra Co atom on the tip apex. Panel (e) shows the image after dropping off the Co atom in the green dotted triangle. The green and pink circles in (c) and (d) mark the tip position in pick-up and drop-off processes, respectively.

atoms in five neighboring clean FHUCs in Fig. 10(a) and converted them into the same faulted bright configuration D through vertical manipulation and *tip-touch* conversion. More importantly, considering the large adsorption energy of Co atoms on Si(111)-(7 × 7), the successful manipulation indicates that our techniques can be applied in many other systems with smaller adsorption energies than Co on Si(111). Up to now, we have demonstrated that the chosen Co/Si(111) system can meet the three prerequisites [1,3,4,17–19] for constructing atomic spin-based devices with the help of our newly developed STM manipulation techniques.

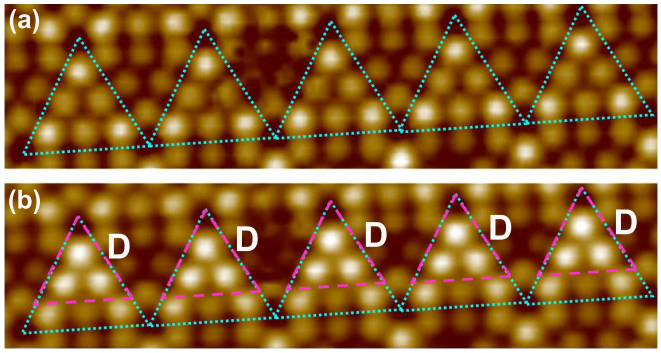

FIG. 10. (Color online) Filled state STM images of the Si(111)-(7 × 7) surface (a) before and (b) after transferring five single Co atoms in the five neighboring clean FHUCs (marked by dotted blue triangles). All five Co atoms are converted into configuration D as highlighted by the dashed pink triangles. The images are taken at $V_s = -0.5$ V and $I = 5$ pA.

IV. CONCLUSION

In conclusion, we have demonstrated that the chosen Co/Si(111)-(7 × 7) system has the potential to become a platform for constructing atomic-scale spin-based devices. A single Co atom on Si(111)-(7 × 7) was discovered to have multiple adsorption sites and in most cases to stay vertically below the outermost silicon layers. Through theoretical computation, the experimentally identified eight adsorption configurations were further found to possess finite spin magnetic moments and represent different spin states. With the combined use of vertical manipulation and the *tip-touch* operation, the position and spin state of single Co atoms were shown to be controllably adjustable. Our demonstrated capability of arranging Co atoms in precise given positions with definitive spins can provide a platform for constructing atomic-scale magnetic structures on semiconductor surfaces. Moreover, we believe our manipulation techniques have wide applications and can be applied to many other systems with adsorption energies comparable or smaller than that of Co atoms on a silicon surface. Our work offers a promising pathway to realize quantum computation and other atomic-scale spin-based devices in a semiconductor matrix.

ACKNOWLEDGMENTS

We gratefully acknowledge fruitful discussions with Professor B. Wang (University of Science and Technology of China). This work was supported by the Research Grants Council of Hong Kong (Grant No. 403311), the Direct Grant for Research from the Chinese University of Hong Kong (Grant No. 4053017), and the MOST 973 Program (Grant No. 2014CB921402).

[1] J. L. O'Brien, S. R. Schofield, M. Y. Simmons, R. G. Clark, A. S. Dzurak, N. J. Curson, B. E. Kane, N. S. McAlpine, M. E. Hawley, and G. W. Brown, Phys. Rev. B **64**, 161401(R) (2001).
[2] S. R. Schofield, N. J. Curson, M. Y. Simmons, F. J. Rueß, T. Hallam, L. Oberbeck, and R. G. Clark, Phys. Rev. Lett. **91**, 136104 (2003).
[3] B. E. Kane, Nature (London) **393**, 133 (1998).
[4] T. D. Ladd, F. Jelezko, R. Laflamme, Y. Nakamura, C. Monroe, and J. L. O'Brien, Nature (London) **464**, 45 (2010).
[5] S. A. Wolf, D. D. Awschalom, R. A. Buhrman, J. M. Daughton, S. von Molnar, M. L. Roukes, A. Y. Chtchelkanova, and D. M. Treger, Science **294**, 1488 (2001).
[6] F. Delgado and J. Fernández-Rossier, Phys. Rev. Lett. **108**, 196602 (2012).
[7] S. Loth, S. Baumann, C. P. Lutz, D. M. Eigler, and A. J. Heinrich, Science **335**, 196 (2012).
[8] R. G. Clark, R. Brenner, T. M. Buehler, V. Chan, N. J. Curson, A. S. Dzurak, E. Gauja, H. S. Goan, A. D. Greentree, T. Hallam, A. R. Hamilton, L. C. L. Hollenberg, D. N. Jamieson, J. C. McCallum, G. J. Milburn, J. L. O'Brien, L. Oberbeck, C. I. Pakes, S. D. Prawer, D. J. Reilly, F. J. Ruess, S. R. Schofield, M. Y. Simmons, F. E. Stanley, R. P. Starrett, C. Wellard, and C. Yang, Philos. Trans. R. Soc. London, Ser. A **361**, 1451 (2003).
[9] Y. Sugimoto, P. Pou, O. Custance, P. Jelinek, M. Abe, R. Perez, and S. Morita, Science **322**, 413 (2008).
[10] Y. Sugimoto, P. Jelinek, P. Pou, M. Abe, S. Morita, R. Perez, and O. Custance, Phys. Rev. Lett. **98**, 106104 (2007).
[11] Y. Sugimoto, A. Yurtsever, M. Abe, S. Morita, M. Ondráček, P. Pou, R. Pérez, and P. Jelinek, ACS Nano **7**, 7370 (2013).
[12] Y. Sugimoto, A. Yurtsever, N. Hirayama, M. Abe, and S. Morita, Nat. Commun. **5**, 4360 (2014).
[13] S. W. Hla, J. Vac. Sci. Technol. B **23**, 1351 (2005).
[14] D. M. Eigler and E. K. Schweizer, Nature (London) **344**, 524 (1990).
[15] C. F. Hirjibehedin, C. P. Lutz, and A. J. Heinrich, Science **312**, 1021 (2006).
[16] A. A. Khajetoorians, J. Wiebe, B. Chilian, and R. Wiesendanger, Science **332**, 1062 (2011).
[17] R. Vrijen, E. Yablonovitch, K. Wang, H. W. Jiang, A. Balandin, V. Roychowdhury, T. Mor, and D. DiVincenzo, Phys. Rev. A **62**, 012306 (2000).
[18] D. Loss and D. P. DiVincenzo, Phys. Rev. A **57**, 120 (1998).
[19] R. Hanson and D. D. Awschalom, Nature (London) **453**, 1043 (2008).
[20] P. A. Bennett, D. G. Cahill, and M. Copel, Phys. Rev. Lett. **73**, 452 (1994).
[21] G. Kresse and J. Hafner, Phys. Rev. B **47**, 558 (1993).
[22] G. Kresse and J. Furthmüller, Phys. Rev. B **54**, 11169 (1996).
[23] M. Affronte, J. Mater. Chem. **19**, 1731 (2009).
[24] T. Balashov, T. Schuh, A. F. Takács, A. Ernst, S. Ostanin, J. Henk, I. Mertig, P. Bruno, T. Miyamachi, S. Suga, and W. Wulfhekel, Phys. Rev. Lett. **102**, 257203 (2009).
[25] C. F. Hirjibehedin, C. Y. Lin, A. F. Otte, M. Ternes, C. P. Lutz, B. A. Jones, and A. J. Heinrich, Science **317**, 1199 (2007).
[26] P. Wahl, P. Simon, L. Diekhöner, V. S. Stepanyuk, P. Bruno, M. A. Schneider, and K. Kern, Phys. Rev. Lett. **98**, 056601 (2007).
[27] N. Néel, R. Berndt, J. Kröger, T. O. Wehling, A. I. Lichtenstein, and M. I. Katsnelson, Phys. Rev. Lett. **107**, 106804 (2011).
[28] D. Wegner, R. Yamachika, X. W. Zhang, Y. Y. Wang, T. Baruah, M. R. Pederson, B. M. Bartlett, J. R. Long, and M. F. Crommie, Phys. Rev. Lett. **103**, 087205 (2009).
[29] B. S. Swartzentruber, Y. W. Mo, M. B. Webb, and M. G. Lagally, J. Vac. Sci. Technol. A **7**, 2901 (1989).
[30] F. F. Ming, K. D. Wang, S. Pan, J. P. Liu, X. Q. Zhang, and X. D. Xiao, ACS Nano **5**, 7608 (2011).
[31] P. E. Blöchl, Phys. Rev. B **50**, 17953 (1994).
[32] Y. Wang and J. P. Perdew, Phys. Rev. B **44**, 13298 (1991).
[33] V. I. Anisimov, J. Zaanen, and O. K. Andersen, Phys. Rev. B **44**, 943 (1991).
[34] S. L. Dudarev, G. A. Botton, S. Y. Savrasov, C. J. Humphreys, and A. P. Sutton, Phys. Rev. B **57**, 1505 (1998).
[35] K. D. Wang, G. Chen, C. Zhang, M. M. Loy and X. D. Xiao, Phys. Rev. Lett. **101**, 266107 (2008).
[36] K. Takayanagi, Y. Tanishiro, S. Takahashi, and M. Takahashi, Surf. Sci. **164**, 367 (1985).
[37] V. I. Anisimov and O. Gunnarsson, Phys. Rev. B **43**, 7570 (1991).
[38] G. K. H. Madsen and P. Novák, Europhys. Lett. **69**, 777 (2005).
[39] H. W. Chang, J. S. Tsay, Y. C. Hung, F. T. Yuan, W. Y. Chan, W. B. Su, C. S. Chang, and Y. D. Yao, J. Appl. Phys. **101**, 09D124 (2007).
[40] J. S. Tsay, Y. D. Yao, and Y. Liou, Surf. Sci. **454**, 856 (2000).